Contribution from the Department of Chemistry,
Princeton University, Princeton, New Jersey 08544

Spectroscopic Study of Chloroiron(II) Complexes in LiCl-DCl-D_2O Solutions

Lynn Vogel Koplitz,* Donald S. McClure, and David A. Crerar†

Received June 27, 1986

The d → d electronic transitions of Fe(II) complexes in LiCl-DCl-D_2O solutions were studied over the concentration range 1-11 *m* Cl^-_{tot} at 25-82 °C. Octahedral species including $Fe(D_2O)_6^{2+}$, $FeCl(D_2O)_5^+$, $FeCl_2(D_2O)_4$, $FeCl_3(D_2O)_3^-$, and $FeCl_4(D_2O)_2^{2-}$ were found to be present over this range as determined by factor analysis and from the rule of the average environment. A low-energy absorption band ($A_{max} \leq 4000$ cm^{-1}) is attributed to the formation of some tetrahedral complex, possibly $FeCl_4^{2-}$, at high temperature, high chloride concentration, or both. A ΔH value of 36-41 kJ/mol was found for the octahedral-tetrahedral equilibrium.

Introduction

Divalent iron exists as the hexaaquo complex in dilute aqueous solution at room temperature as do other first-row transition-metal ions.[1-3] As chloride is added to these solutions, stepwise replacement of H_2O by Cl^- in the metal coordination sphere occurs.[4] Other metal ions, including Mn^{2+},[5] Co^{2+},[6-14] Ni^{2+},[13-15] Cu^{2+},[15] and Zn^{2+},[16,17] have been shown to undergo a coordination change to tetrahedral geometry for conditions of high chloride concentration, high temperature, or both. This study gives evidence for a similar coordination change for Fe^{2+} in acidic D_2O solutions containing varied amounts of LiCl at temperatures up to 82 °C. The formation of mono-, di-, tri-, and tetrachloro octahedral complexes is also postulated. These types of complexes, particularly the tetrahedral ones, are believed to be important in stabilizing dissolved metals relative to precipitated phases in naturally occurring hydrothermal solutions.[18,19]

Previous work on Fe^{2+} complexes includes studies of $FeCl_4^{2-}$ in melts,[20] crystals[21-24,56] and nonaqueous solutions.[21,23] Several authors have investigated aqueous solution equilibria at room temperature,[25-28] and higher T,[14,29] as well. $FeCl_4^{2-}$ was not found in water solutions. Other studies of complexes for a series of divalent first-row transition metals conspicuously exclude Fe^{2+}.[9,29-32]

Lithium chloride and D_2O were used to access a wide range of chloride concentration and to extend the observable wavelength range. The d → d transitions of interest occur in the near-IR region for Fe^{2+}. Combination and overtone bands of water also occur in this region,[33,34] precluding any absorption measurements for Fe^{2+} at wavelengths greater than about 1360 nm (in a 1-cm cell). D_2O extends this range down to about 1860 nm. With 1- or 0.1-mm cells and D_2O, usable spectra to 2500 nm were obtained. Our initial experiments using up to 5 *m* NaCl and 72 °C showed no evidence of $FeCl_4^{2-}$ (see Results and Discussion section), while the more concentrated LiCl solutions showed the interesting results reported here.

Experimental Section

Equipment. All spectra were obtained with a Varian 2390 UV-vis-NIR scanning double-beam spectrophotometer. An IEEE-488 interface to an Apple IIe computer facilitated digital data collection. Spectra were transmitted to Princeton's IBM 3081 mainframe for computational analyses.

The sample cells in most runs were 1-cm path length, thick-walled Infrasil fused-silica cuvettes with Teflon stoppers. In other runs, stoppered 1-mm and demountable 0.1-mm cells were used (NSG Precision Cells). A thermostated cell base, supplied by Varian, allowed temperature control by water circulation. Heating, cooling, and pumping of the water through the cell holder were accomplished with a Polyscience Model 90T constant temperature circulator. Temperatures, measured by $^1/_{32}$-in. type K thermocouples wedged snugly between the cuvette and holder walls and displayed by an Omega 410B Digicator, were constant to within 0.1 °C.

The sample, monochromator, and detector compartments of the spectrophotometer were purged with clean, dry nitrogen.

Sample Preparation. All solutions were prepared by dissolving electrolytic iron wire (99.998% pure, 1.0 mm diameter, Aldrich) in 37 wt% DCl in D_2O (Aldrich) under an inert (Ar) atmosphere with gentle warming. Deoxygenated D_2O (99.8 atom % D, Aldrich) was added to this concentrated solution to yield the desired iron concentration. Two separate solution series were prepared. Each solution in series A contained 0.10 *m* Fe^{2+} and 1.12 *m* DCl with 0.00, 3.71, 5.73, and 9.07 *m* LiCl added. Series B contained 0.053 *m* Fe^{2+} and 1.02 *m* DCl with 0.00, 0.92, 2.02, 3.01, 4.39, 5.49, 6.01, 6.95, 7.95, 9.03, and 9.84 *m* LiCl added. In this way solutions of approximately 1, 2, 3, 4, 5, 6, 7, 8, 9, 10, and 11 *m* total Cl^- were obtained. Reference solutions were prepared similarly, matching the sample LiCl and DCl concentrations as closely as possible. Analogous 0.060 and 0.60 *m* Fe^{2+} solutions were made for use with the 1- and 0.1-mm cells. All molalities are with respect to weight of D_2O.

* To whom correspondence is to be addressed at Chemistry Department, Pomona College, Claremont, CA 91711.
† Department of Geological and Geophysical Sciences, Princeton University, Princeton, NJ 08544.

(1) Holmes, O. G.; McClure, D. S. *J. Chem. Phys.* **1957**, *26*, 1686.
(2) George, P.; McClure, D. S. *Prog. Inorg. Chem.* **1959**, *1*, 381.
(3) Apted, M. J.; Waychunas, G. A.; Brown, G. E. *Geochim. Cosmochim. Acta* **1985**, *49*, 2081.
(4) Bjerrum, J. *Chem. Rev.* **1950**, *40*, 381.
(5) Vogel, L. M. Ph.D. Thesis, Princeton University, 1986.
(6) Bjerrum, J.; Halonin, A. S.; Skibsted, L. H. *Acta Chem. Scand., Ser. A* **1975**, *A29*, 326.
(7) Zeltmann, A. H.; Matwiyoff, N. A.; Morgan, L. O. *J. Phys. Chem.* **1968**, *72*, 121.
(8) Cotton, F. A.; Goodgame, D. M. L.; Goodgame, M. *J. Am. Chem. Soc.* **1961**, *83*, 4690.
(9) Libus, Z. *Pol. J. Chem.* **1979**, *53*, 1971.
(10) Swaddle, T. W.; Fabes, L. *Can. J. Chem.* **1980**, *58*, 1418.
(11) Scaife, D. E.; Wood, K. P. *Inorg. Chem.* **1967**, *6*, 358.
(12) Krauss, U.; Lehmann, G. *Ber. Bunsen-Ges. Phys. Chem.* **1972**, *76*, 1066.
(13) Lüdemann, H. D.; Franck, E. U. *Ber. Bunsen-Ges. Phys. Chem.* **1967**, *71*, 455; **1968**, *72*, 514.
(14) Susak, N. J.; Crerar, D. A. *Geochim. Cosmochim. Acta* **1985**, *49*, 555.
(15) Angell, C. A.; Gruen, D. M. *J. Am. Chem. Soc.* **1966**, *88*, 5192.
(16) Beer, J.; Crow, D. R.; Grzeskowiak, R.; Turner, I. D. M. *Inorg. Nucl. Chem. Lett.* **1973**, *9*, 35.
(17) Kanno, H.; Hiraishi, J. *J. Raman Spectrosc.* **1980**, *9*, 85.
(18) Susak, N. J.; Crerar, D. A. *Econ. Geol.* **1982**, *77*, 476.
(19) Crearar, D. A.; Susak, N. J.; Borcsik, M.; Schwartz, S. *Geochim. Cosmochim. Acta* **1978**, *42*, 1427.
(20) Gruen, D. M.; McBeth, R. L. *Pure Appl. Chem.* **1963**, *6*, 23.
(21) Furlani, C.; Cervone, E.; Valenti, V. *J. Inorg. Nucl. Chem.* **1963**, *25*, 159.
(22) Gibb, T. C.; Greenwood, N. N. *International Atomic Energy Agency Tech. Rep. Ser.*—I. A. E. A. **1966**, *No. 50*.
(23) Gill, N. S. *J. Chem. Soc. A* **1961**, 3512.
(24) Clark, R. J. H.; Nyholm, R. S.; Taylor, F. B. *J. Chem. Soc. A* **1967**, 1802.
(25) Johnson, G. K.; Bauman, J. E., Jr. *Inorg. Chem.* **1978**, *17*, 2774.
(26) Kanno, H.; Hiraishi, J. *J. Raman Spectrosc.* **1982**, *12*, 224.
(27) Raman, S. *J. Inorg. Nucl. Chem.* **1976**, *38*, 1741.
(28) Vincze, L.; Kraut, B.; Papp, S. *Inorg. Chim. Acta* **1984**, *85*, 89.
(29) Bird, B. D.; Day, P. *Chem. Commun.* **1967**, 741.
(30) Libus, Z.; Tialowska, H. *J. Solution Chem.* **1975**, *4*, 1011.
(31) Bird, B. D.; Briat, B.; Day, P.; Rivoal, J. C. *Symp. Faraday Soc.* **1969**, *No. 3*.
(32) Gill, N. S.; Nyholm, R. S. *J. Chem. Soc. A* **1959**, 3997.
(33) Waggener, W. C.; Weinberger, A. J.; Stoughton, R. W. *Oak Ridge Natl. Lab., [Rep] ORNL (U.S.)* **1965**, *ORNL-3832, UC-4-Chemistry*.
(34) Buback, M.; Crerar, D. A.; Koplitz, L. V. *Hydrothermal Experimental Techniques*; Ulmer, G. C., Barnes, H. L., Eds.; Wiley-Interscience: New York, 1987; Chapter 14.

0020-1669/87/1326-0308$01.50/0

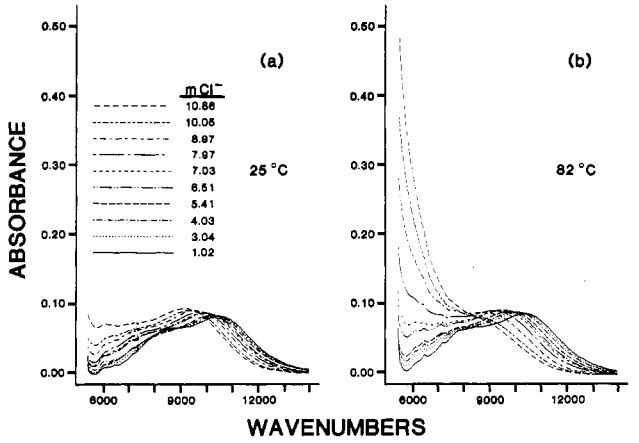

Figure 1. Spectra of series B solutions at constant temperature. $[Fe^{2+}] = 0.053$ *m*.

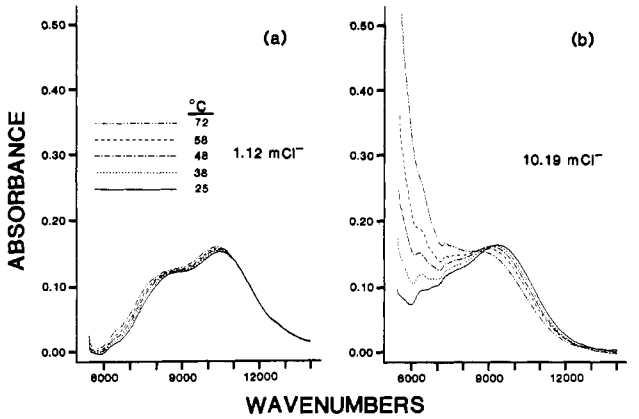

Figure 2. Spectra of series A solutions with (a) lowest and (b) highest $[Cl^-]$ at varied T. $[Fe^{2+}] = 0.10$ *m*.

The LiCl was stored in a hot oven to keep it dry. All mixing was carried out in a nitrogen-filled glovebag, where the samples were then stored prior to use.

Measurements. Spectra were recorded at temperatures of 24.6 ± 0.1, 38.1 ± 0.1, 48.4 ± 0.1, 57.9 ± 0.1, and 71.7 ± 0.2 °C for series A and 24.5 ± 0.1, 49.3 ± 0.2, 71.0 ± 0.2, and 82.4 ± 0.2 °C for series B, 64 spectra in all. (Here temperature ranges indicate total variation for all samples near a given temperature. Each individual sample was constant to ±0.1 °C.) Samples were always handled under nitrogen to avoid oxygen and H_2O contamination. Measurements were made as soon as possible after sample preparation, usually within a day.

The amount of Fe^{3+} formed was gauged approximately from Cl^- to Fe^{3+} charge-transfer bands in the UV spectra.[5,35] Generally about 2–3% of the iron was oxidized for a normal set of spectra taken from 25 to 82 °C (about 5 h). In no case did the amount of Fe^{3+} exceed 10%. Near-IR spectra for solutions that were cooled back down to 25 °C always matched the first spectrum for that solution very closely.

Results and Discussion

Figures 1 and 2 show representative spectra taken at constant temperature for varied chloride concentration (Figure 1) or constant chloride concentration and varied temperature (Figure 2). The most noteworthy features of these spectra are (1) the increased absorbance at low energy for the most concentrated chloride solutions relative to the other solutions at constant temperature, (2) the red shift in the band maximum from 10 500 cm^{-1} at 25 °C and 1 *m* total chloride to about 8500 cm^{-1} at 82 °C and 11 *m* total chloride, (3) the slight increase in absorbance maximum with increasing $[Cl^-]$ at constant *T* (Figure 1a), and (4) the small incremental decrease in absorbance near 9500 cm^{-1}, which corresponds to a larger incremental increase in intensity at long wavelengths with each step up in *T* (Figure 2b). As discussed below, all of these observations are consistent with the formation

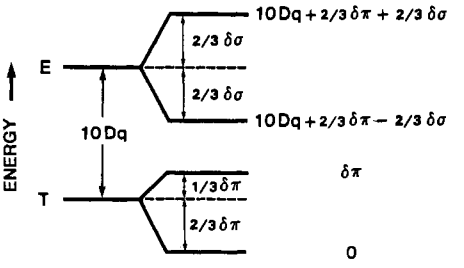

Figure 3. Qualitative energy level diagram for $FeCl(D_2O)_5^+$.

of higher chloride ligation number (n_{Cl^-}) octahedral complexes and, at high enough $[Cl^-]$ and *T*, tetrahedral complexes.

Octahedral Complexes. At 25 °C in dilute aqueous solution, solvated Fe^{2+} exists as the octahedral hexaaquo complex.[1,3] The only spin-allowed d → d transition for this complex appears in the near-IR with $\epsilon_{max} \approx 1.6$ at 10 500 cm^{-1}.[34,36] The excited state of the complex is Jahn–Teller distorted so that the $^5T_{2g} \rightarrow {}^5E_g$ transition, which corresponds directly to 10*Dq* for a d^6 ion, splits into two components separated by about 2300 cm^{-1}.[34,36-38] When this splitting is corrected for, a value of about 9350 cm^{-1} can be assigned to 10*Dq*.

Octahedral complexes where one (or more) of the water ligands has been replaced by Cl^- will have spectra similar to that of the hexaaquo ion. The Jahn–Teller effect will be converted gradually to a tetragonal splitting as the parameters of the substituent depart from those of H_2O. One could think of this change as a stabilization of one Jahn–Teller minimum relative to the others. In the $^5T_{2g}$ ground state the effects of the substituent on the vibronic levels will be smaller than in the excited state and need not concern us here. A crude description of the energy levels of a monosubstituted complex is given in Figure 3 and will help to interpret the spectra. In chloroaquo complexes the magnitude of 10*Dq* will be slightly less than that of the hexaaquo ion since Cl^- is a weaker field splitter than H_2O.[39] The extinction coefficient could be higher since the complex is no longer of strictly octahedral symmetry and the parity forbiddenness of the d → d transition is therefore relaxed. But in fact, as shown in Figure 1a, there is only a very slight increase in ϵ_{max}.

The Number of Octahedral Species Present. By using principal factor analysis (PFA) it is possible to determine the number of absorbing species in a series of solutions from absorbance data. A thorough, detailed explanation of this technique is given by Malinowski and Howery.[40] Briefly, using Beer's Law, we can express the absorbance, *A*, at any wavelength, *i*, for any solution, *k*, as the sum of the absorbances for all the components, *j*, present in that solution, as

$$A_{ik} = \sum_{j=1}^{n} \epsilon_{ij} C_{jk} \qquad (1)$$

where ϵ is an extinction coefficient and *C* is a concentration. This expression represents a set of equations involving a linear sum of products and should, therefore, be factor analyzable. The number of absorbing components present in a set of solutions is determined by first constructing a matrix of absorbance values such that each column represents the spectrum for a solution and each row index is a wavelength. The covariance matrix, formed by premultiplying this absorbance matrix by its transpose, is then diagonalized to obtain a set of eigenvalues and eigenfunctions that exactly reproduce the original data matrix. The eigenfunctions, or factors, associated with the smallest eigenvalues are then systematically eliminated since they serve only to reproduce error. When the remaining set of factors reproduces the original data matrix within experimental error, the number of principal components is the number of factors left.

(35) Gamlen, G. A.; Jordan, D. O. *J. Chem. Soc. A* **1953**, 1435.
(36) Cotton, F. A.; Myers, M. D. *J. Am. Chem. Soc.* **1960**, *82*, 5023.
(37) Jones, G. D. *Phys. Rev.* **1967**, *155*, 259.
(38) Hatfield, W. E.; Piper, T. S. *Inorg. Chem.* **1964**, *3*, 1295.
(39) Jørgensen, C. K. *Inorganic Complexes*; Academic: New York, 1963.
(40) Malinowski, E. R.; Howery, D. G. *Factor Analysis in Chemistry*; Wiley-Interscience: New York, 1980.

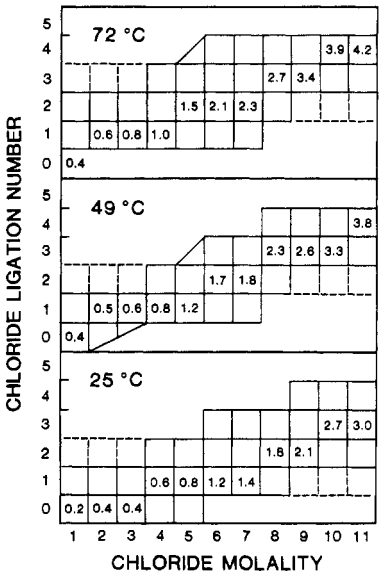

Figure 4. Summary of the results of principal factor analysis. Numbers in the boxes indicate average chloride ligation number determined from the absorbance maximum and Figure 6. Diagonal lines represent ambiguous analyses. Dashed lines are complexes whose presence cannot be determined from our data.

This goal was accomplished by applying the program FACTANAL[41] to appropriate sets of spectra at a given T and using Malinowski's error analysis methods[40] to determine how many factors belong to the primary set. For example, nine spectra from solution series A and B with $[Cl^-]$ ranging from 5 to 11 m at 71.5 ± 0.5 °C were factor analyzed. Only wavelengths between 800 and 1200 nm were used in order to avoid contributions from solvent absorbance. Four components were found to be present. After the spectra for solutions of $[Cl^-] < 8$ m were removed, the remaining five spectra were similarly analyzed. Now only three factors were identified. By this method of varying the members of the spectra set, the number of octahedral complexes contributing to most of the spectra could be mapped out. The results of PFA are summarized in Figure 4. Successive replacement of D_2O by Cl^- is assumed.

Note that diagonal block boundaries in Figure 4 indicate ambiguous results. For example, it could not be ascertained whether the 5 m Cl^- solution at 49 °C contained two or three octahedral complexes. The dashed lines indicate that the presence of that complex could not be confirmed or denied for that temperature. This limitation arises since factor analysis requires at least as many data sets (i.e. spectra) as there are factors.[40]

From Figure 4 we can see that the kinds of octahedral complexes present shift toward higher n_{Cl^-} at lower Cl^- molality as T increases. At 49 °C, $Fe(D_2O)_6^{2+}$ has disappeared in solutions where $[Cl^-] \geq 4$ m. At 72 °C that complex is not significant even in the 1 m Cl^- solution. $[FeCl_4(D_2O)_2]^{2-}$, the complex with the highest n_{Cl^-} at 4, appears only above 8 m Cl^- at 25 °C while it is already formed in solutions of about 5 m Cl^- at 72 °C.

Individual Component Spectra. In addition to finding the number of species present by factor analysis, it is theoretically possible to determine the spectrum for each species as well as its concentration in each solution. In the matrix representation of eq 1

$$[A] = [\epsilon][C]$$

each column of $[A]$ is an experimentally obtained spectrum for solution k and each column of $[\epsilon]$ is the extinction coefficient function, or spectrum, of component j. The column indices for $[C]$ are the solutions, k, so that each entry in a row of $[C]$ gives the concentration of a particular component in a given solution.

(41) Program 320, Quantum Chemistry Program Exchange, Indiana University, Bloomington, IN, 1976.

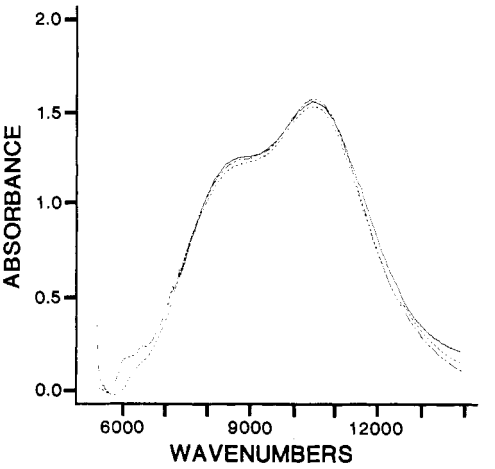

Figure 5. 25 °C spectra of the ~1 m Cl^- solutions of series A (--) and B (----), and 0.5 m $FeSO_4 \cdot 6H_2O$ in 0.1 N H_2SO_4 (—). All spectra were scaled to $[Fe^{2+}] = 1$ m.

In fact, the problem is already solved in this form, but $[\epsilon]$ and $[C]$ do not represent physically significant extinction coefficients or concentrations. A final nontrivial step using methods such as target transformation or rotation[40] is required to reach this highly desirable end. We have not yet accomplished this last step with our own data.

Another method for determining extinction coefficient functions for individual solution components involves non-linear regression fits to absorbance data. Equation 1 can be rewritten in terms of stability quotients as

$$A_{ik} = \sum_{j=1}^{n} \epsilon_{ij}\beta_j[M]_k[L]_k^j \qquad (1a)$$

where

$$\beta_j = \frac{[ML_j]}{[M][L]^j}$$

and square brackets indicate the free concentration of that component. A program written by Leggett[42] uses estimates of β_j and ϵ_{ij} values for a selection of appropriate species to fit experimental absorbance data according to eq 1a by incrementing these parameters to minimize the differences between calculated and observed spectra. This program, SQUAD, has been used successfully by Seward to determine the UV spectra and stability constants of chlorolead(II) complexes in aqueous solution up to 300 °C.[43] Our own attempts to apply this program to our Fe^{2+} data, for wavelengths less than 1200 nm where solvent structure interference could be excluded, failed. This failure is probably primarily due to the appreciable overlap of the component spectra as we now go on to show.

Estimation of the Spectrum of the Monochloro Complex. In this section we employ known and estimable changes in d → d transition energies and bandshapes in order to construct a spectrum for $FeCl(D_2O)_5^+$. This hypothetical spectrum turns out to be remarkably similar to that of $Fe(D_2O)_6^{2+}$.

The spectra of our 1 m Cl^- solutions very closely resemble that of $Fe(H_2O)_6^{2+}$ as shown in Figure 5. Published formation constants for $FeCl(H_2O)_5^+$ cover the range 0.29–4.45 at 25 °C,[44-46] requiring 23–82% $FeCl(D_2O)_5^{2+}$ in these 1 m Cl^- solutions. However, the spectra shown in Figure 5 give no indications of a species other than $Fe(D_2O)_6^{2+}$. For the monochloro complex the difference in σ- and π-antibonding character of the ligands splits the states such that two electronic transitions differing by $^4/_3\delta\sigma$

(42) Leggett, D. J. *Anal. Chem.* **1977**, *49*, 276.
(43) Seward, T. M. *Geochim. Cosmochim. Acta* **1984**, *48*, 121.
(44) Wells, C. F.; Salam, M. A. *Nature (London)* **1964**, *203*, 751.
(45) Olerup, H. Ph.D. Thesis, Lund, Sweden, 1944.
(46) Raman, S. *J. Inorg. Nucl. Chem.* **1976**, *38*, 1741.

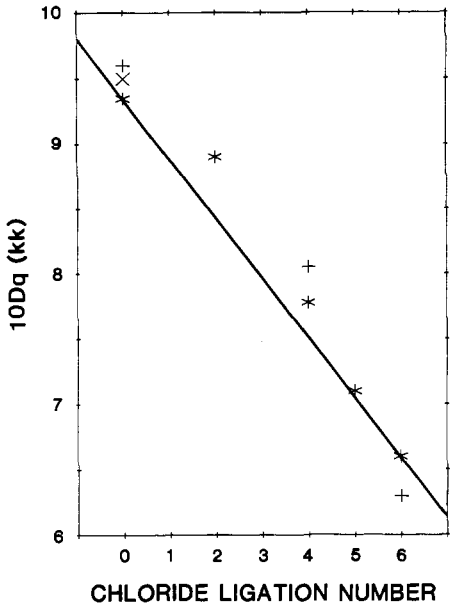

Figure 6. $10Dq$ as a function of chloride ligation number. Literature sources for the plotted values $n_{Cl^-} = 0$, (×, +) ref 36, (*) ref 34; $n_{Cl^-} = 2$, ref 48; $n_{Cl^-} = 4$, (+) ref 49 and 50, (*) ref 48; $n_{Cl^-} = 5$, ref 48; $n_{Cl^-} = 6$, (*) ref 49, (+) ref 37.

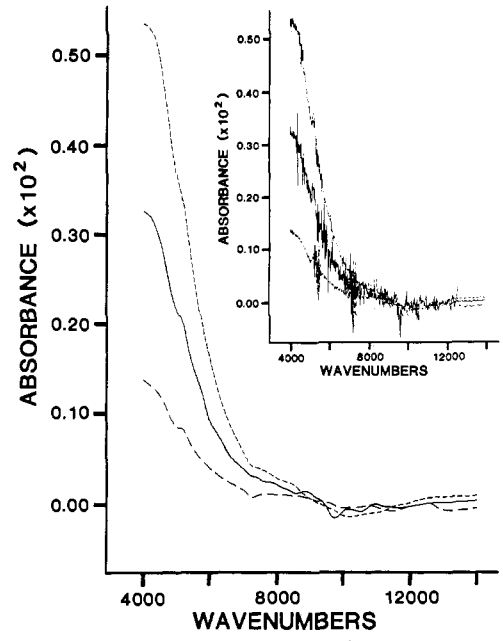

Figure 7. Difference spectra for a 0.06 *m* Fe^{2+}, 9 *m* Cl^- solution taken in 1-mm cells: (--) 80–25 °C; (—) 66–25 °C; (– –) 49–25 °C. Data were smoothed by using a spline technique. Inset shows unsmoothed data.

($\delta\sigma = \sigma_{Cl^-} - \sigma_{H_2O}$) result (see Figure 3).[47] We need values for $\delta\sigma$, $\delta\pi$ and $10Dq$ in order to simulate the monochloro complex spectrum.

One way to estimate $10Dq$ for a mixed-ligand complex is by comparing it with crystals and melts of known metal coordination. If we plot $10Dq$ vs. n_{Cl^-} for the homocoordinate complexes ($Fe(H_2O)_6^{2+}$ and $FeCl_6^{4-}$) and interpolate between them, the $10Dq$ values for the series of sequentially substituted complexes should fall close to that line. Jørgensen refers to this as the rule of the average environment.[39] Such a plot of Fe^{2+} in crystals containing Cl^- and H_2O, and in aqueous solution, is shown in Figure 6. The intermediate heterocomplexes do indeed fall near the line interpolated from $Fe(H_2O)_6^{2+}$(aq) to $FeCl_2$ (anhydrous). From Figure 6 we find $10Dq = 9000$ cm^{-1} for $FeCl(D_2O)_5^+$.

We can get estimates of $\delta\sigma$ and $\delta\pi$ from the spectrum of crystalline $FeCl_2 \cdot 4H_2O$, which contains *trans*-dichloroiron centers, and Figure 6. The energy levels of the *trans*-dichloro complex will also split as shown in Figure 3 but to twice that extent. The crystal spectrum consists of two major bands[48] at 6800 and 11 000 cm^{-1} so that ${}^8/_3\delta\sigma = 4200$ cm^{-1}. The difference between the average energy of these observed transitions and the value of $10Dq$ predicted by Figure 6 corresponds to ${}^4/_3\delta\pi$ or 400 cm^{-1}.

Combining all of this information we predict that $FeCl(D_2O)_5^+$ should exhibit two bands at $10Dq + {}^2/_3\delta\pi - {}^2/_3\delta\sigma = 8150$ cm^{-1} and $10Dq + {}^2/_3\delta\pi + {}^2/_3\delta\sigma = 10\,250$ cm^{-1}. This hypothetical spectrum is red-shifted by 250 cm^{-1} from the hexaaquo spectrum at the high-energy band maximum and by 50 cm^{-1} for the low-energy band. Since the whole Jahn–Teller split hexaaquo band is about 4000 cm^{-1} wide at half-maximum height, these are very small relative changes. Provided that the extinction coefficients are also very similar for these complexes, the SQUAD program would have difficulty separating their contributions to the solution spectra, giving unsatisfactory, nonunique fits.

Average Chloride Ligation Numbers of the Dominant Complexes. Even though we cannot at present map out the individual component spectra, we can determine chloride ligation numbers by supposing that A_{max} for a solution closely corresponds to A_{max} for the dominant octahedral complex in that solution. At 25 °C the 11 *m* Cl^- solution in series B exhibits A_{max} at 9175 cm^{-1} (see Figure 1a). Taking 1150 cm^{-1}, one-half the Jahn–Teller splitting in $Fe(H_2O)_6^{2+}$, as a rough estimate for the band-splitting correction we get $10Dq \approx 8025$ cm^{-1}, which corresponds to $n_{Cl^-} = 3$ on Figure 6. The spectrum of the 10 *m* Cl^- solution at 72 °C from series A, as plotted in Figure 2b, has a barely discernible maximum at about 8620 cm^{-1}; with the approximate splitting correction, $10Dq \approx 7470$ cm^{-1} and $n_{Cl^-} \approx 4$. This type of empirical analysis leads us to the conclusion that $[FeCl_4(D_2O)_2]^{2-}$ is dominant at very high $[Cl^-]$ and $T = 72$ °C.

Average chloride ligation numbers found in this manner are shown in the appropriate box in the PFA summary (Figure 6), nicely illustrating the agreement between these two independent methods of inferring the presence of the different octahedral complexes. Discrepancies do occur at 72 °C. Here PFA does not indicate the presence of $Fe(D_2O)_6^{2+}$ for $[Cl^-] \leq 3$ *m*, but the spectrum maximum mapped onto Figure 6 gives $n_{Cl^-} < 1$, which is only possible if some fraction of the iron is $Fe(D_2O)_6^{2+}$. Also, $n_{Cl^-} = 4.3$ for the 11 *m* Cl^- solution, requiring the presence of complexes with $n_{Cl^-} > 4$ while the PFA results give a maximum of $n_{Cl^-} = 4$.

Our simple method of mapping energies of absorbance maxima onto Figure 6 does not account for changes in $10Dq$ or band splitting with temperature. Since $10Dq$ depends inversely upon the metal-to-ligand distance, which will increase with temperature,[51] we would expect the analogous $10Dq$ vs. n_{Cl^-} diagram at 72 °C to indicate a lower n_{Cl^-} for any given $10Dq$. Then the n_{Cl^-} found by using the 25 °C graph (Figure 6) would be higher than the actual value. On the other hand, splitting will probably increase with temperature[52] so that the correction that has been used is too low. Then the value of $10Dq$ that was used is too high, resulting in an artificially low n_{Cl^-}. We can approximately gauge these opposing effects for the hexaaquo complex from Figure 2a. While the splitting increases by ~200 cm^{-1} and $10Dq$ decreases by ~270 cm^{-1} these changes do not affect our conclusions significantly, only increasing n_{Cl^-} about 0.1.

Tetrahedral Complexes. A tetrahedral Fe^{2+} complex will also exhibit only one spin-allowed transition, ${}^5E \rightarrow {}^5T_2$, at about ${}^4/_9$ the energy of the ${}^5T_{2g} \rightarrow {}^5E_g$ transition in a similar octahedron[51] (i.e. same ligands). Therefore, we might predict $10Dq$ to be about

(47) McClure, D. S. In *Proceedings of the Sixth International Conference on Coordination Chemstry*; Macmillan: New York, 1961; pp 498–509.
(48) Burbridge, C. D.; Goodgame, D. M. L. *J. Chem. Soc. A* **1968**, 1410.
(49) Winter, G. *Aust. J. Chem.* **1968**, *21*, 2859.
(50) Lawson, K. E. *J. Chem. Phys.* **1966**, *44*, 4159.
(51) Dunn, T. M.; McClure, D. S.; Pearson, R. G. *Some Aspects of Crystal Field Theory*; Harper and Row: New York, 1965.
(52) Freeman, T. E.; Jones, G. D. *Phys. Rev.* **1969**, *182*, 411.

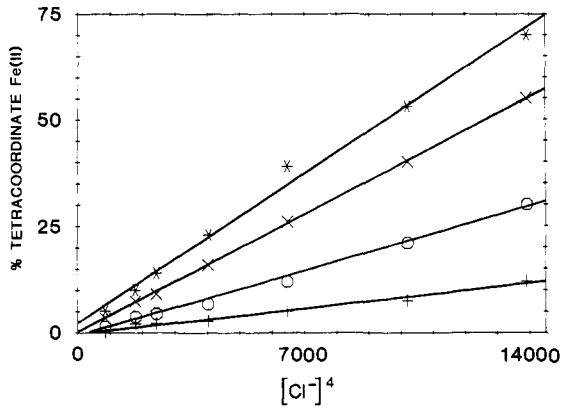

Figure 8. Percent conversion to the tetrahedral complex vs. $[Cl^-]^4$ as determined from A_{1800nm} for series B solutions: (+) 25 °C; (O) 49 °C; (×) 72 °C; (*) 82 °C.

4160 cm^{-1} for a hypothetical tetrahedral $Fe(H_2O)_4^{2+}$ complex. Gruen and McBeth[20] found an absorbance band with A_{max} at ~4080 cm^{-1} for tetrahedral $FeCl_4^{2-}$ (Fe^{2+} substituted for Zn^{2+} in a Cs_2ZnCl_4 crystal). The $^5E \rightarrow {}^5T$ transition for a tetrahedral complex such as $[FeCl_n(H_2O)_m]^{2-n}$ should therefore lie near 4100 cm^{-1}. Extinction coefficients for tetrahedral complexes are generally about 10–100 times greater than those of similar octahedra.[8,53] Gruen and McBeth give $\epsilon_{max} \approx 26$ for $FeCl_4^{2-}$ which is about 16 times the ϵ_{max} value of 1.6 for $Fe(H_2O)_6^{2+}$.

By using 1-mm path length cells and D_2O, we can scan into the near-IR as far as 4000 cm^{-1} where solvent absorption prevents further observation. Figure 7 shows difference spectra for a 0.06 *m* Fe^{2+}, 9 *m* Cl^- solution where, in order to correct for systematic errors, the 25 °C spectrum has been subtracted from those at 49, 66 and 80 °C. A band that appears to approach its maximum at the solvent transmission limit becomes more intense with increasing *T*. The *apparent* extinction coefficient is about $(0.053/0.06) \times 10 \approx 9$ at 4000 cm^{-1} and 80 °C, assuming all the iron to be tetrahedrally coordinated. If ϵ_{max} is closer to 26 as Gruen and McBeth[20] found, then approximately 38% of the total iron is converted to the tetrahedral complex.

Similar spectra were obtained in 0.1-mm cells for 0.6 *m* Fe^{2+} solutions. Here it was possible to scan the entire range of the instrument down to 3170 cm^{-1}. However, the strong solvent bands dominate the spectra below 4000 cm^{-1}, and no additional information concerning Fe^{2+} absorption can be gained. We found that these 0.1-mm path length spectra are entirely coincident with 1-mm cell spectra for the same *T* and $[Cl^-]$.

In summary, we observe a new band located at or below 4000 cm^{-1} whose $\epsilon_{max} > 9$. We attribute this new absorption to a tetrahedral complex $[FeCl_n(D_2O)_m]^{2-n}$. We can observe the tail of this band above 5375 cm^{-1} in a 1-cm cell more conveniently and with a better signal-to-noise ratio (see Figure 1 and 2). This longer path length also allows simultaneous monitoring of the weaker octahedral bands. Since the absorbance in the region 5300–5600 cm^{-1} changes in proportion to A_{2500nm} in the 1-mm cell spectra, the absorbance at 5556 cm^{-1} (1800 nm) in the 1-cm cell data is representative of the tetrahedral complex. The ratio of absorbance at 4000 cm^{-1} to that at 5556 cm^{-1} is 2.25 ± 0.05 at all temperatures.

It is difficult to derive a thermodynamic equilibrium constant from our data, but as a practical matter it would be useful to know the fraction of Fe^{2+} converted to the tetrahedral complex at a given temperature and DCl and LiCl concentrations. This could be found from the absorbance if we knew the extinction coefficients of $FeCl_4^{2-}$. As an approximation we have taken the value of ϵ_{max} for Cs_2ZnCl_4:Fe^{2+} from the paper of Gruen and McBeth[20] to be the value of the extinction coefficient for our solution spectrum at 4000 cm^{-1}. We have used the absorbance ratio $A_{2500}/A_{1800} = 2.25 \pm 0.5$ to find the extinction coefficient at 1800 nm and thus

(53) Ballhausen, C. J.; Liehr, A. D. *J. Mol. Spectrosc.* **1958**, *2*, 342.

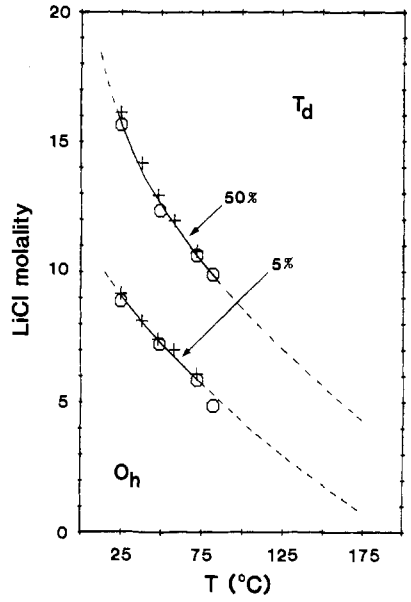

Figure 9. Temperature/chloride concentration zones of predominance for octahedral and tetrahedral coordination of Fe^{2+} in LiCl–DCl–D_2O as demarcated by 5% or 50% conversion to the tetrahedral form. Points were determined from Figure 8 (O) and a similar plot of series A data (+). Dotted lines are extrapolations.

the concentration of $FeCl_4^{2-}$. The fractional conversions obtained in this way look reasonable when compared to the decrease of the octahedral species absorption bands. For example, at 72 °C in 10.19 *m* LiCl and 0.10 *m* Fe^{2+}, the conversion is calculated to be 30%. The band due to all the octahedral species is reduced considerably in area although an exact percent decrease cannot be found because of band overlap.

Figure 8 shows the percent conversion for several temperatures plotted as a function of $[Cl^-]^4$. These plots at a given temperature are remarkably linear as if a simple mass action law based on concentration were operating, suggesting $Fe(D_2O)_6^{2+} + 4Cl^- \rightleftarrows FeCl_4^{2-} + 6D_2O$ as the important overall equilibrium.

It is of particular interest to geochemists to know the stability fields of these different complexes at higher temperatures.[14] Figure 9 depicts concentration and temperature zones of predominance for the octahedral and tetrahedral Fe^{2+} complexes as demarcated by 5% or 50% conversion to the tetrahedral form. The points were calculated by using the linear relationship between $[Cl^-]^4$ and percent conversion at a given temperature from Figure 8 and an analogous plot of series A data. It is easy to imagine a smooth extrapolation of these curves to higher and lower temperatures as shown by the dotted lines. Susak's estimates for the conversion boundary fall about 3 or 4 *m* lower than our 5% line at any given temperature.[14]

Estimation of Enthalpy of Formation of the Tetrahedral Complex. An approximate value of ΔH for the formation of the tetrahedral complex from octahedral precursors in solution can be found from the temperature dependence of the corresponding absorption bands. The "tetrahedral" band between 3950 and 6600 cm^{-1} shows the strongest response to chloride concentration as well as the greatest response to temperature. The octahedral band region shows complicated $[Cl^-]$ and temperature response due to the successive formation of octahedral aquochloro complexes. It is difficult to find a region of this spectrum from which to determine the formation of the tetrahedral complex by the depletion of the octahedral complexes. It is not possible at present to decide which equilibrium constant is being most affected by temperature changes. The strong temperature dependence of the tetrahedral band is therefore simply attributed to an equilibrium between six-coordinate and four-coordinate Fe^{2+} ions.

Let αc represent the concentration of tetrahedral Fe^{2+} and $(1 - \alpha)c$ that of octahedral species. The major temperature effect observed is in the tetrahedral band, which measures αc. We took the absorbances at 940 nm to represent $(1 - \alpha)c$. Then the ΔH

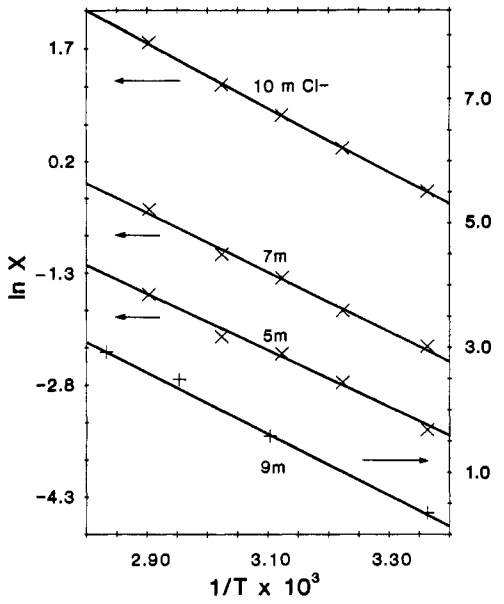

Figure 10. ln X, where $X = A_{1800}/A_{940}$ on the left ordinate and $X = A_{2500}/A_{940}$ on the right ordinate, vs. $1/T \times 10^3$ (K^{-1}): (+) 1-mm cell data shown in Figure 7; (×) series A solution data. Slopes of these lines give $-\Delta H/R$.

we report will be the temperature coefficient of ln $(\alpha/(1-\alpha))$, which is proportional to ln $[A_\lambda/A_{940}]$ measured as just stated. Therefore we give

$$\Delta H = -R \frac{\mathrm{d}}{\mathrm{d}(1/T)} \ln \left[\frac{A_\lambda}{A_{940}} \right]$$

where A_λ will be the absorbance between 6600 and 3950 cm^{-1}. A plot of ln (A_{1800}/A_{940}) vs. $1/T$ is closely linear from 25 to 82 °C and its slope gives $\Delta H = 36$ kJ/mol. Figure 10 shows such a plot for several chloride concentrations. The data at 2500 nm taken in 1-mm cells yields a temperature dependence that gives $\Delta H = 41$ kJ/mol.

The absorbance is proportional to the concentration, but the proportionality factor (ϵ) may be a function of temperature if the band shape changes with temperature. To estimate the effect of temperature on the tetrahedral band shape we used the configuration coordinate model,[54] which gives the bandwidth as a function of temperature for a Gaussian band as

$$\sigma(T) = \sigma(0)\ [\coth\ (\hbar\omega/2kT)]^2$$

The vibration frequency was taken to be 266 cm^{-1}, a value found for the symmetric mode in the Raman spectrum of $FeCl_4^{2-}$.[55] For a nominal bandwidth of 2000 cm^{-1} at 25 °C, the band broadens to 2650 cm^{-1} at 82 °C. A red shift of 200 cm^{-1} was also included to take account of the decrease in $10Dq$,[51] and the band areas were taken to be constant. The low- and high-temperature curves cross near the half-maximum point on the high-energy side. This point corresponds to about 1800 nm in our data, showing that there should be no correction for the band broadening effect here. At wavelengths closer to the band maximum the band broadening reduces the extinction coefficient by at most 20%. This is small compared to the effect of the chemical equilibrium on the concentration change.

Another contribution to the temperature effect could be caused by the movement of the solvent band at 1900 nm. This could affect the data in the region of 1800 nm, but not the data between the solvent bands from 4200 to 5000 cm^{-1}. Comparison of the results obtained for the two regions show that there is no appreciable error from this source.

Comparison with Co^{2+} and Ni^{2+}. While some limited studies of Fe^{2+} complexation in aqueous chloride solutions have been published,[1,14,19,25-28] extensive literature exists for Co^{2+} [6-14] and Ni^{2+}.[9,11,13-15,30] These latter two ions are more conveniently studied spectroscopically than Fe^{2+} since they are not rapidly oxidized by air and their d → d spectra are not severely occluded by solvent bands. Fe^{2+} is closely associated with Co^{2+} and Ni^{2+} in its periodic properties, and we may expect certain similarities in complexation behavior.

Table I summarizes some published results concerning $O_h \rightarrow T_d$ equilibria for these ions. It can be seen that our ΔH value for Fe^{2+} in LiCl-DCl-D_2O is consistent with most of these findings.

Table I. Enthalpies of Reaction Reported in the Literature for Octahedral-Tetrahedral Equilibria

equilibrium	ΔH, kJ/mol	ref
$NiCl_6^{4-} \rightleftharpoons NiCl_4^{2-} + 2Cl^-$	35.6 ± 1.3	15
$CoCl_2(H_2O)_4 + Cl^- \rightleftharpoons CoCl_3(H_2O)^- + 3H_2O$	49.0	11
$Co(H_2O)_6^{2+} + 4Cl^- \rightleftharpoons CoCl_4^{2-} + 6H_2O$	46	12
$Co(H_2O)_nCl_m + pCl^- \rightleftharpoons CoCl_4^{2-} + nH_2O$[a]	62 ± 2	10
$Co(H_2O)_6^{2+} \rightleftharpoons Co(H_2O)_4^{2+} + 2H_2O$	16.6 ± 2.0	10
$Fe(D_2O)_nCl_m + pCl^- \rightleftharpoons Fe(D_2O)_qCl_r + (n-q)D_2O$[b]	36-41	this work

[a] $n + m = 6$; $m + p = 4$. [b] $n + m = 6$; $q + r = 4$; $r = m + p$.

Summary

From the analysis of ligand field spectra for Fe^{2+} in acidic LiCl-D_2O solutions, both octahedral and tetrahedral complexes are apparently present for $25 \leq T \leq 82$ °C. Higher chloride ligation numbers are favored by increasing T, [Cl^-], or both. The dominant octahedral complex(es) for conditions where a low-energy absorbance appears, which is attributable to tetrahedral species, are probably $[FeCl_4(D_2O)_2]^{2-}$ and $[FeCl_3(D_2O)_3]^-$. The limiting tetrahedral complex in our experiments is probably $FeCl_4^{2-}$. The enthalpy change for the $O_h \rightarrow T_d$ equilibrium was found to be approximately 36-41 kJ/mol, a range in accord with that reported by other investigators for Co^{2+} and Ni^{2+} under similar conditions.

Acknowledgment. The authors thank the NSF (Grant No. CHE-8506943), The Shell Foundation, and the Geological Society of America for generous support. We are also grateful to Brent Koplitz for drafting many of the figures.

(54) Sturge, M. D. *Solid State Phys.* **1967**, *29*.
(55) Avery, J. S.; Burbridge, C. D.; Goodgame, D. M. L. *Spectrochim. Acta, Part A* **1968**, *24A*, 1721.
(56) Briat, B.; Canit, J. C. *Mol. Phys.* **1985**, *48*, 33.